Materials Research Proceedings 41 (2024) 1686-1695 https://doi.org/10.21741/9781644903131-187

In-situ CT of the clinching process – Influence of settling effects due to process interruptions

KÖHLER Daniel[a]*, KUPFER Robert[b], TROSCHITZ Juliane[c] and GUDE Maik[d]

Institute of Lightweight Engineering and Polymer Technology, TUD Dresden University of Technology, Germany

[a]daniel.koehler3@tu-dresden.de, [b]robert.kupfer@tu-dresden.de,
[c]juliane.troschitz@tu-dresden.de, [d]maik.gude@tu-dresden.de

Keywords: Clinching, Testing, Computed Tomography, In-Situ CT

Abstract. In lightweight constructions, clinching represents a cost-effective solution, in which joints are produced by local cold forming of the joining parts. Clinching phenomena are typically evaluated using destructive testing methods. While these methods influence the clinch point's state, in-situ computed tomography (in-situ CT) is able to explore the clinching process with a specimen under load. Here, the path-controlled clinching process is interrupted at certain displacement levels and the specimen is scanned by CT while remaining in a stationary state. These interruptions are always accompanied by settling effects reducing the reaction force. Therefore, in this work, the influence of these interruptions on the force-displacement behavior during clinching and on the final clinch point's geometric properties is investigated.

Introduction

Clinching technology. The increased interest in lightweight components for car body constructions requires joining methods, which are able to join different materials. Likewise, in light of ever-increasing legal requirements on material recycling [1], joining solutions that facilitate material separation with low contamination [2] are gaining increasing interest. In terms of joining lightweight materials such as aluminum, clinching poses a good alternative to bolting, riveting or bonding with high strength adhesives as it allows a good recyclability. This is achieved because a force and form fit joint is created by locally deforming two join partners without requiring any auxiliary joining elements [3]. Moreover, different materials can be joined [4], and the costs can be reduced to 30 - 60 % compared to resistance spot welding [5].

Designing clinch points. The design of clinch points is described in DVS/EFB 3420 [6], providing reference values for quasi-static shear strength based on individual material-thickness combinations. However, in practice, joint design often relies on experience, iterative testing, and tool revisions [7]. This results in a tool configuration which is specific to a single material-thickness combination often leading to an unnecessary material utilization. To enhance the design and adapt clinch tools more efficiently to varying conditions, a better understanding of occurring phenomena in the clinch point is necessary. Besides that, a more precise investigation of the phenomena can also facilitate an accurate validation of numerical models which are also required for the design process.

Classical characterization methods. Intuitively, phenomena occurring during the clinching process are visually or optically inspected after manufacturing [8]. This way, asymmetries and peripheral cracks can be found, however phenomena in depth remain unknown. Using destructive metallographic examination according to [8], deformation phenomena within the clinch point can be visualized. For this, the specimen is cut close to the cross-section of interest, then it is embedded in resin, ground, and optionally polished. A macroscopic analysis of the cross section enables the determination of geometric parameters such as undercut and neck thickness, as well as asymmetries and cracks within the cutting plane. Additionally, this method reveals the interface

and outer edges of the clinch point in the respective cross-section, which is often utilized for validating numerical models [9]. In order to understand the evolution of phenomena, clinch points can be tested and analyzed in step-setting tests [10]. Here, a series of metallographic examinations is conducted with clinch points which were manufactured at different stages of the clinching process. However, this way, phenomena such as closing cracks and springback effects influence the investigated displacement state. Furthermore, investigations at stages when no sufficient undercut is created are hardly possible. But most importantly, the investigation of the evolution of particular phenomena is restrained due to material and manufacturing variations.

In-situ CT. As an alternative, X-ray in-situ computed tomography (in-situ CT) allows the three-dimensional visualization of clinching phenomena under load. Hence, the evolution of individual phenomena can be investigated. For this, a CT system is combined with a testing machine mounted with CT suitable clinching tools. Applying this method using a lab-based CT system, the specimen is clinched stepwise in increasing displacement levels. Usually, at each displacement level, the testing process is interrupted, and the specimen is rested in order to allow a CT scan of the specimen's displacement state. These interruptions are accompanied by settling effects reducing the reaction force measured by the testing machine over the resting time. Optionally, X-ray in-situ CT with synchrotron X-ray source allows scanning time of the order of seconds or below [11]. This could enable CT investigations of continuous clinching processes, though at a significantly decreased manufacturing speed (common clinching speed: 2 mm/s). Because of the high scanning costs of synchrotron CT, lab-based X-ray in-situ CT remain a popular alternative and shall be investigated in this work.

The lab-based in-situ CT method has been gaining increased interest over the last decade [12]. It was already applied to investigating aluminum foams under tensile loading [13] or metal ceramic composites in compression tests [14]. In terms of joints, shear tests of adhesively bonded riveted lap joints [15] or the pull out behavior of inserts out of carbon fiber reinforced plastic [16] were already investigated by in-situ CT. Moreover, the in-situ CT of the manufacturing and testing process of clinch points was introduced in [17] and [18], respectively. However, to the author's knowledge, there are no published investigations on the influence of the interruptions, which are inherent for lab-based in-situ CT, on the clinching process or comparable high deformation processes. So far, it is usually assumed that the settling effects have no significant impact on the process of interest. In order to clarify on this potential impact a more detailed investigation is required.

Hence, in this work, two set of specimens are investigated. First, the specimens are clinched continuously (Conti), second the specimens are clinched with longer interruptions (StopGo) at several displacement levels. The force-displacement behavior is analyzed and the geometric properties of the final clinch point is compared statistically.

Materials and Methods

Experimental setup. For the experiments, clinch points made of two 2 mm thick aluminum round sheets (ø 40 mm) are produced in two different manufacturing procedures in the same in-situ CT clinching setup. For reference, continuous clinching is conducted for ten specimens with a cross beam displacement rate of 2 mm/s (Conti specimen set). Here the punch is moved to a total displacement. After that the punch is instantly withdrawn resulting in a bottom thickness of 0.70±0.01. Another ten specimens (StopGo specimen set) are clinched using the same total punch displacement. To represent the in-situ CT process, the punch movement is interrupted and held in position for 15 min at distinctive displacement levels in different phases of the clinching process. It was interrupted at 25 % (offsetting phase), 50 % (upsetting phase), 75 % (upsetting phase) and 100 % (flow pressing phase) of the total punch displacement (stop points). A preload of 1.7 kN is chosen to align the experiments at a force occurring shortly after the punch touched the sheets.

Evaluation of the force displacement behavior. First, it is tested how well the force-displacement curves of both manufacturing procedures align. This is done through statistically testing for a significant deviation. For this, the force, the normalized standard deviation of the forces, and the normalized differences between the means of the forces of both procedures are investigated over the displacement. Comparing the forces, clear deviations at the stop points are expected due to settling effects in the StopGo tests. Therefore, it is investigated how well the forces of both procedures align shortly after the stop point. This is done by testing the deviation between both procedures statistically for significance at a displacement of 0.2 mm after each stop point (evaluation point). Additionally, the maximum forces are evaluated statistically. For comparing both manufacturing procedures, both mean values (t-test) and variances (F-test) of the investigated forces at the evaluation points and the maximum forces are tested for homogeneity. Thus, it shall be verified that the force displacement curves of both procedures do not deviate from each other significantly.

Evaluation of the final geometry. Furthermore, it is verified whether the final geometries of the respective specimen sets align. This is done by statistically testing whether the specimen sets' geometry deviate from each other significantly. For this purpose, the clinch points are analyzed using (ex-situ) CT (cf. scanning parameters in Table 1). Here, a stack of six specimens mounted in a specimen holder is scanned using the CT system V|TOME|X L450[1] [2] with a helix scanning trajectory. After the scans are reconstructed using the Feldkamp algorithm in phoenix datos|x 2 Reconstruction[3], the volumes are edited in VG Studio Max 3.4[4]. For the evaluation, the specimens' surfaces are to be compared. The surface of each specimen is determined by first creating a contour based on the iso 50 value and excluding wrongly detected voids and noise particles. Then, this contour is used as a starting contour to determine the maximum grey value gradient within an area of 10 µm, which is used as the surface to be analyzed.

For the evaluation, the specimens' surfaces are to be compared. The surface of each specimen is determined by first creating a contour based on the iso 50 value and excluding wrongly detected voids and noise particles. Then, this contour is used as a starting contour to determine the maximum grey value gradient within an area of 10 µm, which is used as the surface to be analyzed. For comparing the contours, the bottom thickness is measured along the rotation axis of a fitted cone (cf. Figure 1). The neck thicknesses are measured horizontally (cf. translated surface in Figure 1) in at a constant distance of 2.45 mm to a fitted surface on the die faced sheet surface (cf. fitted surface in Figure 1)) in the cross section planes 0° and 90° relative to the material texture of both sheets[5]. The neck thicknesses are then evaluated for the 0° and 90° cross section planes respectively.

The neck thicknesses are then evaluated for the 0° and 90° cross section planes respectively. For verifying that the final geometries do not deviate significantly, the mean values (t-test) and variances (F-test) of the neck and bottom thicknesses for both specimen sets are evaluated.

[1] GE Sensing & Inspection Technologies GmbH
[2] 300 kV microfocus, flat detector with pixel size 200 x 200 µm, 2016 x 2016 pixels, 16 bit
[3] GE Sensing & Inspection Technologies GmbH
[4] Volume Graphics GmbH, Heidelberg, Deutschland
[5] Prior clinching the sheets are positioned towards each other with aligned texture orientation

Table 1: Applied parameters for the CT measurement and image analysis

Parameter	Unit	Value
Acceleration voltage	[kV]	150
Tube current	[µA]	80
X-ray projections		2016
Exposure time	[ms]	500
Voxel size	[µm]	10
Skip		1
Averaging		5
Physical filter	[mm]	1 (Cu)
Focal spot size	[µm]	12

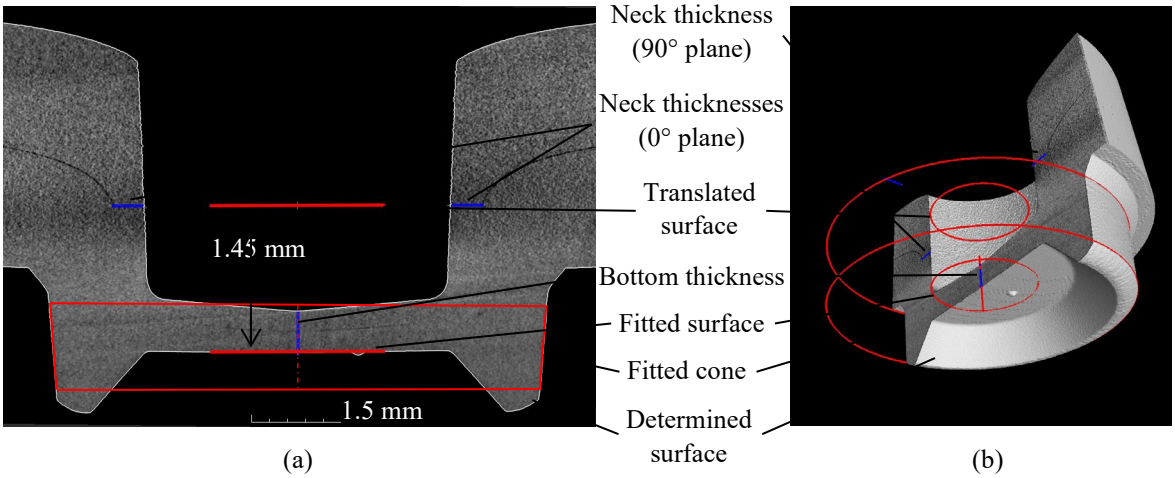

Figure 1: 0° cross section of the clinch point CT volume in 2D (a) and 3D (b) with the fitted geometries supporting the measurement of geometric properties in the final clinch point.

Results and Discussion

Force-displacement evaluation. The force-displacement diagrams for both sample variations are shown in Figure 1. The stop points, evaluation points, and close-up views of the graphs at these points can be seen. A notable observation is the significant deviation of one curve, C04_A_CV_440[6], from the StopGo tests. Aside from that, after each stop point the forces of both procedures align well, though the StopGo graphs show a decreasing alignment to the Conti graphs with increasing displacement level. Evaluating Figure 2 supports the identification of specimen C04_A_CV_440 as an outlier (boxplot method). Therefore, this specimen is excluded from the statistical analysis. In the boxplots, it can be seen that the variances and the mean of both specimen sets seem to be similar at all evaluation points.

[6] Unified specimen notation in Collaborative Research Center TRR285

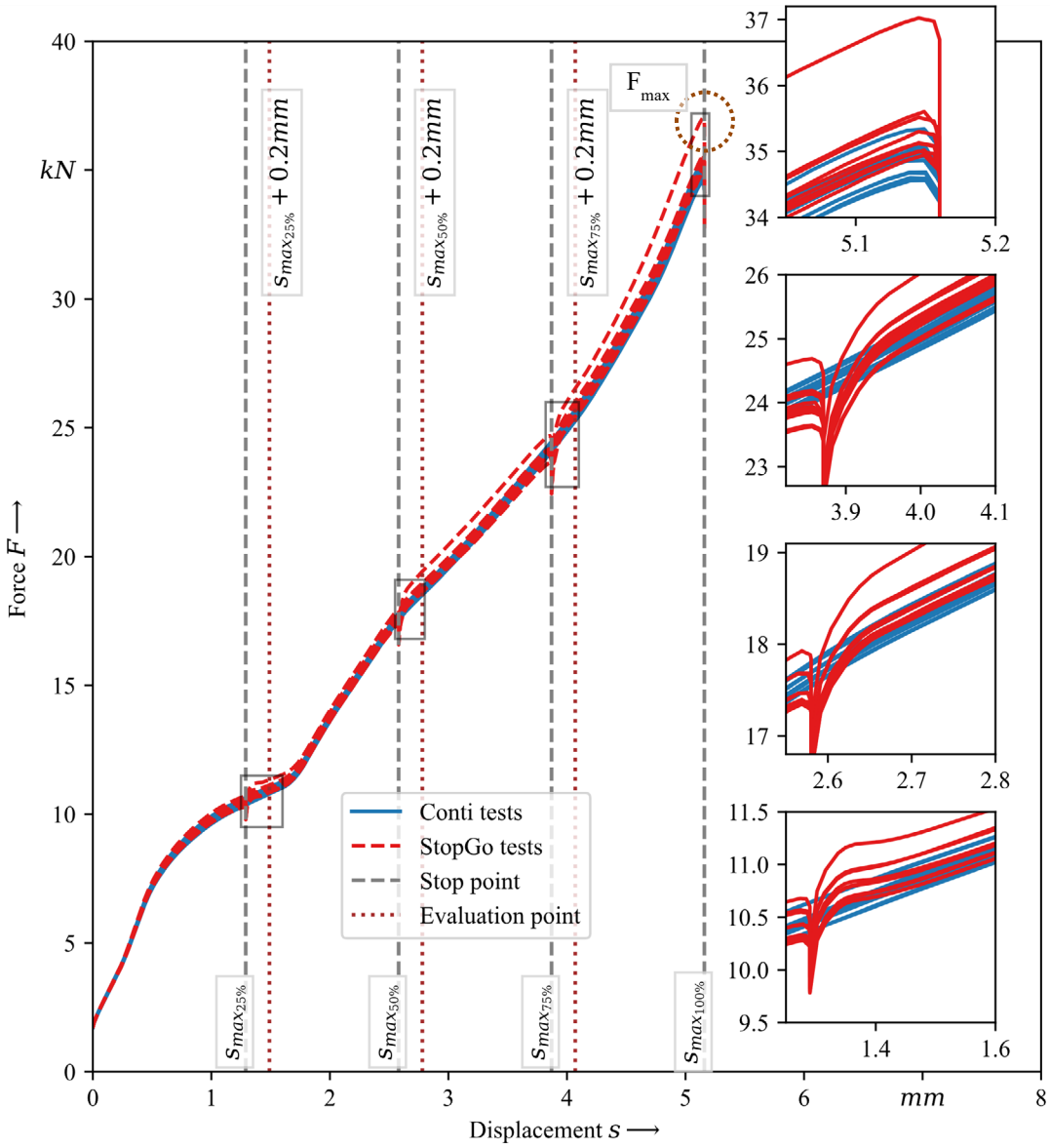

Figure 2: Force-displacement diagram of Conti and StopGo tests with the stop points and the evaluated points

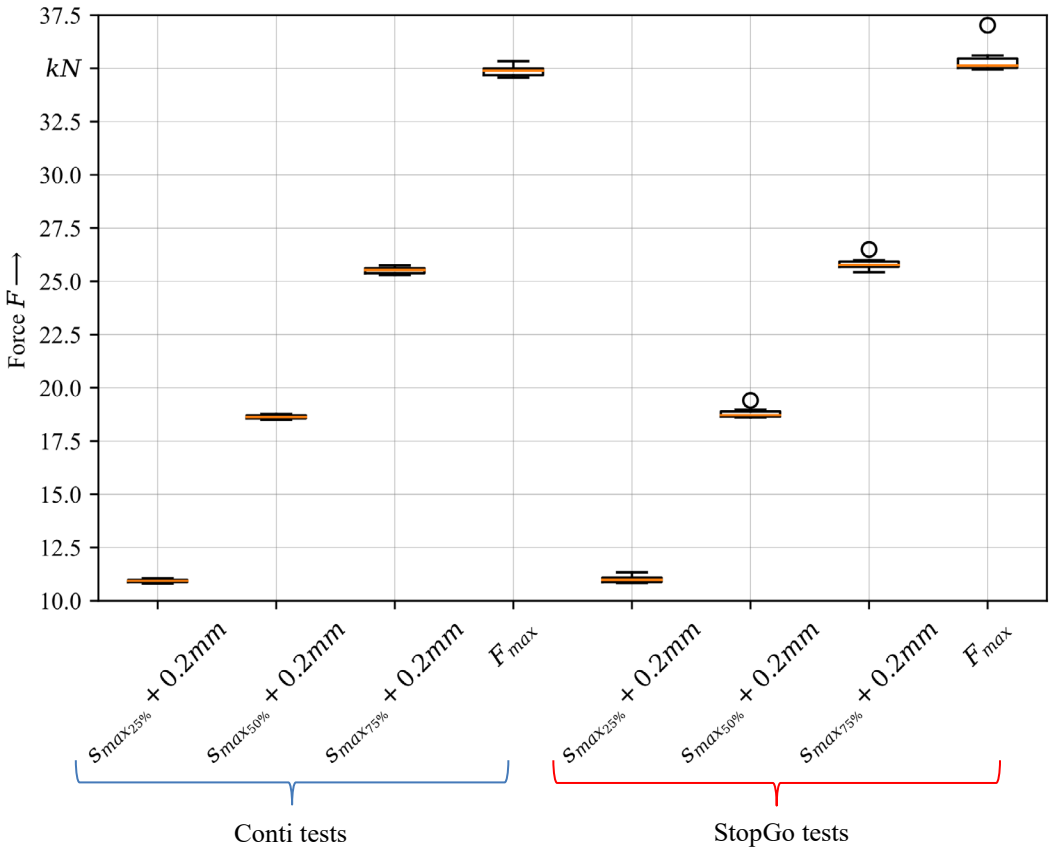

Figure 3: Box plot diagrams at the evaluation points and F_{max}

In Figure 4 a, the normalized standard deviations of both manufacturing procedures over the displacement are displayed. Before the first stop point, no difference can be seen. After the first stop point an increasing variance is notable for the StopGo procedure. However, near the maximum force both variances are similar again. In light of the maximum normalized standard deviation of 1 %, it seems that both procedures exhibit similarly low deviations over the whole process. The forces at the evaluation points were checked for normal distribution (Shapiro-Wilk and Anderson-Darling test) and the F-test was conducted (test for variance homogeneity). In Table 2 the results for each evaluation point are shown. In a one-tailed test, it is tested whether StopGo tests exhibit a significantly higher variance as Conti tests. It can be concluded that the variance is not significantly different (min p-value 0.2312 > 0.05). Consequently, no significant impact of the interruptions on the variance of the forces can be found.

To get an impression of the mean value homogeneity, the averaged force at each displacement is calculated resulting in a respresentive force-displacement plot for each specimen set. The normalized[7] difference between the averaged StopGo and Conti graphs gives an impression of the mean value homogeneity (cf. Figure 3 b). It can be seen that the normalized mean force difference before the first stop point is below 0.7 %. The stop points cause a high difference in the mean value due to the drop in force caused by settling effects. After the stop point, the differences in the mean value decrease. However, the rate of decline is slowing down after each stop point. Shortly before the maximum force, the difference reduces to 0.5 %. Overall, the differences are at a relatively low level. Conducting the t-test (test for mean homogeneity) at the evaluation points reveals a

[7] using the averaged Conti graph

decreasing p-value with increasing displacement. A significant deviation (α = 0.05) is found for the evaluation point $s_{max_{75\%}} + 0.2\ mm$ and F_{max}.

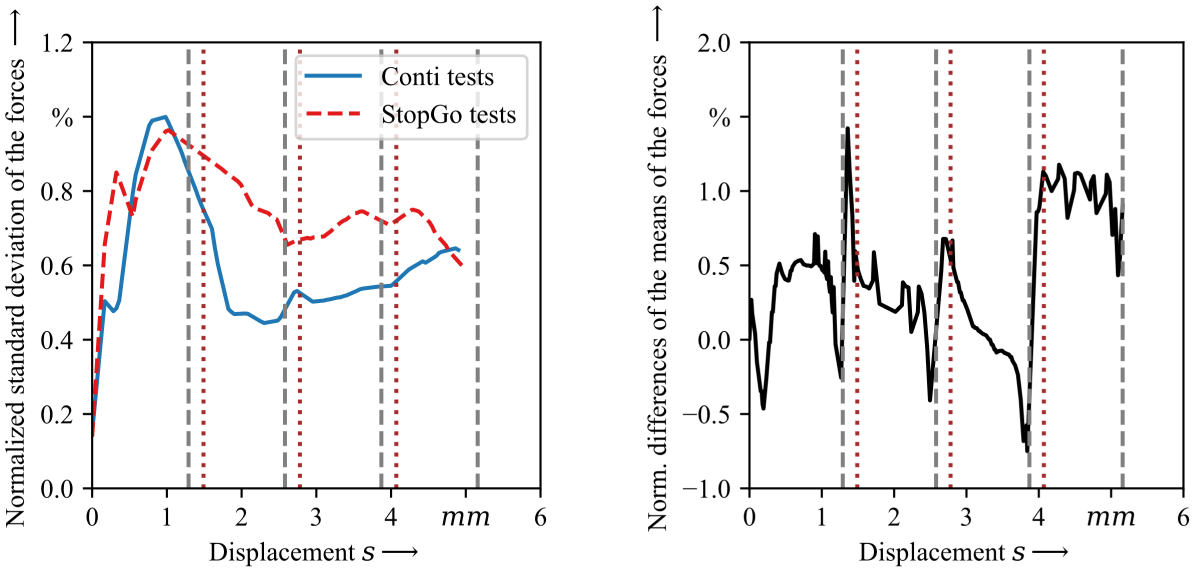

Figure 4: The normalized standard deviation of both procedures over the displacement (a). Normalized differences of the means of the forces of both procedures over the displacement (b). Outlier excluded.

Table 2: F- and t-test results for the evaluation of the force-displacement behavior (outlier excluded)

Test method	Evaluated point	Statistic	p-value	Significant deviation (p-values > 0.05)
F-test	$s_{max_{25\%}} + 0.2\ mm$	1.58	0.2649	Wrong
	$s_{max_{50\%}} + 0.2\ mm$	1.64	0.2476	Wrong
	$s_{max_{75\%}} + 0.2\ mm$	1.70	0.2312	Wrong
	F_{max}	0.958	0.5291	Wrong
t-test	$s_{max_{25\%}} + 0.2\ mm$	-0.59	0.5600	Wrong
	$s_{max_{50\%}} + 0.2\ mm$	-1.88	0.0773	Wrong
	$s_{max_{75\%}} + 0.2\ mm$	-2.71	0.0146	True
	F_{max}	-2.86	0.0108	True

Geometry evaluation. The box plots for the investigated geometric properties are shown in Figure 4. The bottom thickness clearly deviates between both specimen sets. At the neck thickness, no obvious deviations can be seen in between the specimen sets. However, a clear difference can be seen when comparing the results from the 0° and 90° cross section plane for both specimen sets. Evaluating the F- and t-test, it can be seen that all investigated properties have no significant variance inhomogeneity. However, the mean values of the bottom thickness deviate significantly in between both specimen sets.

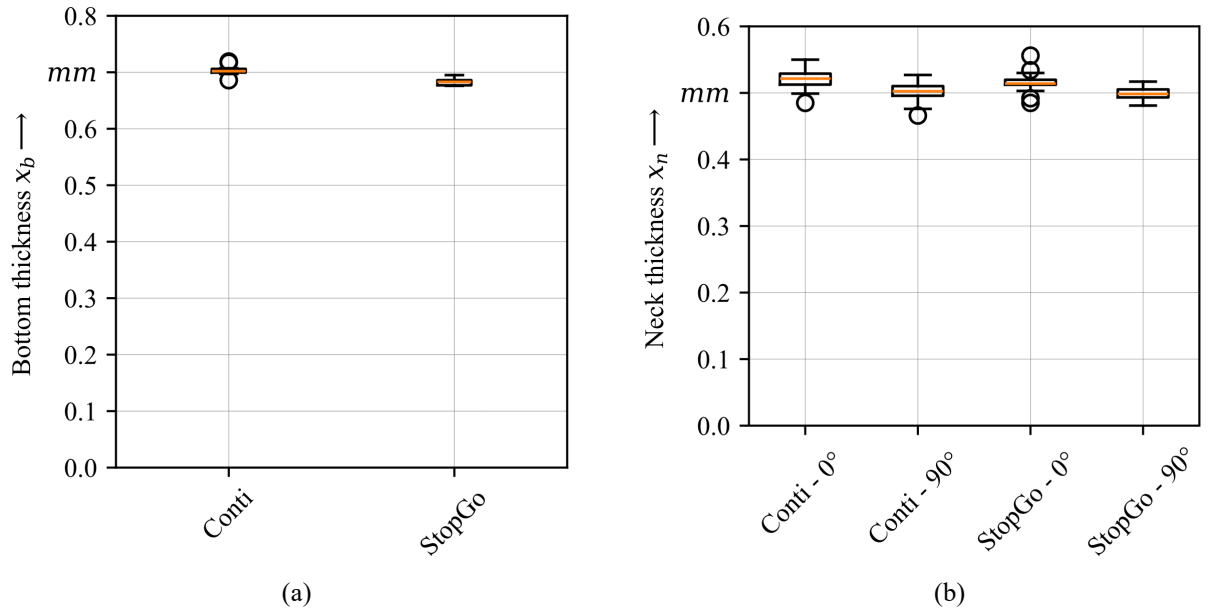

Figure 5: Measured bottom thickness (a) and neck thicknesses in the respective cross section planes (b) for both specimen sets.

Table 3: F- and t-test results for the evaluation of the geometry (outlier excluded)

Test method	Evaluated point	Statistic	p-value	Significant deviation (p-values > 0.05)
F-test	Bottom thickness x_b	0.43	0.8798	Wrong
	Neck thickness x_b 0°	0.77	0.7078	Wrong
	Neck thickness x_b 90°	0.47	0.9383	Wrong
t-test	Bottom thickness x_b	5.44	4.35E-05	True
	Neck thickness x_b 0°	0.51	0.6064	Wrong
	Neck thickness x_b 90°	0.80	0.4244	Wrong

Summary and Conclusions

Investigating the deformation phenomena during clinching processes can preferably be done using in-situ CT as this method does not influence the process compared to destructive methods. When conducting a lab-based in-situ CT investigation, the clinch point is created stepwise. At displacement levels of interest, the process is interrupted and the specimen is scanned by CT while remaining in a stationary state. These interruptions are always accompanied by reductions of the reaction force caused by settling effects. While this investigation method is already applied to clinching and also to other processes, the effect of interrupting the process of interest is not investigated in detail yet. Therefore, in this work, the clinching forces of interrupted and continuous clinching processes as well as the resulting geometry of the clinch point are compared statistically. While the variances of these properties of both clinching procedures are well aligned, the mean values at higher clinching forces and of the bottom thicknesses deviated significantly. At the stepwise processes the mean clinching force is higher and the mean bottom thickness is smaller. However, the differences are relatively low. The means and the variances of the neck thicknesses of both specimen sets did not deviate significantly.

It can be concluded that performing a clinching process with interruptions as it is common in in-situ CT investigations has a relatively small but partly significant impact on the resulting clinching forces and geometric properties of the clinch point. At the continuous tests, the punch is directly withdrawn after reaching the final punch displacement in contrast to the stepwise test. Thus, the differences in the bottom thickness can be explained by settling effects during the interruption at the last stop point leaving a higher plastic deformation.

Considering the small differences in reaction forces and geometric properties it can be concluded that an in-situ CT investigation can sufficiently accurately represent the continuous clinching process. Thus, with this method, important phenomena and the evolvement of the final geometry can be analyzed. For a further alignment of the geometric properties, particularly the bottom thickness, the in-situ CT clinching process needs to be adapted, potentially by reducing the total punch displacement.

References

[1] European Commission, "A European Strategy for Plastics in a Circular Economy: Communication from the Commission to the European Parliament, the Council, the European Economic and Social Committee and the Committee of the Regions," Brussels, Jan. 2018. Accessed: Mar. 20 2022. [Online]. Available: https://ec.europa.eu/environment/circular-economy/pdf/plastics-strategy.pdf

[2] K. Ragaert, L. Delva, and K. van Geem, "Mechanical and chemical recycling of solid plastic waste," *Waste management (New York, N.Y.)*, vol. 69, pp. 24–58, 2017. https://doi.org/10.1016/j.wasman.2017.07.044

[3] V. K. Soo, P. Compston, and M. Doolan, "The influence of joint technologies on ELV recyclability," *Waste management (New York, N.Y.)*, vol. 68, pp. 421–433, 2017. https://doi.org/10.1016/j.wasman.2017.07.020.

[4] X. He, "Clinching for sheet materials," *Science and technology of advanced materials*, vol. 18, no. 1, pp. 381–405, 2017. https://doi.org/10.1080/14686996.2017.1320930

[5] P. Kovács and M. Tisza, "Investigation of clinch joints made of similar and dissimilar materials," *IOP Conf. Ser.: Mater. Sci. Eng.*, vol. 426, p. 12028, 2018. https://doi.org/10.1088/1757-899X/426/1/012028

[6] *Technical Bulletin DVS 3420: Prüfung der Eigenschaften mechanisch und kombiniert mittels Kleben gefertigter Verbindungen*, 3420, Working Group V10 "Mechanical Joining" by the joint committee for DVS and EFB, Düsseldorf, Jun. 2021.

[7] G. Meschut and F. F. Menne, *Automatisierte Variantenreduzierung durch virtuelle Verbindungsauslegung beim Halbhohlstanznieten,* 1st ed. Aachen: Shaker Verlag, 2018.

[8] *Testing of properties of joints - Testing of properties of mechanical and hybrid (mechanical/bonded) joints: Prüfung der Eigenschaften mechanisch und kombiniert mittels Kleben gefertigter Verbindungen*, 3480-1, Working Group V10 "Mechanical Joining" by the joint committee for DVS and EFB, Düsseldorf, Dec. 2007.

[9] S. Coppieters, S. Cooreman, P. Lava, H. Sol, P. van Houtte, and D. Debruyne, "Reproducing the experimental pull-out and shear strength of clinched sheet metal connections using FEA," *Int J Mater Form*, vol. 4, no. 4, pp. 429–440, 2011. https://doi.org/10.1007/s12289-010-1023-6

[10] R. Kupfer *et al.,* "Clinching of Aluminum Materials – Methods for the Continuous Characterization of Process, Microstructure and Properties," *Journal of Advanced Joining Processes*, vol. 5, p. 100108, 2022. https://doi.org/10.1016/j.jajp.2022.100108

[11] J. Dewanckele, M. A. Boone, F. Coppens, D. van Loo, and A. P. Merkle, "Innovations in laboratory-based dynamic micro-CT to accelerate in situ research," *Journal of microscopy*, vol. 277, no. 3, pp. 197–209, 2020. https://doi.org/10.1111/jmi.12879

[12] E. A. Zwanenburg, M. A. Williams, and J. M. Warnett, "Review of high-speed imaging with lab-based x-ray computed tomography," *Meas. Sci. Technol.*, vol. 33, no. 1, p. 12003, 2022. https://doi.org/10.1088/1361-6501/ac354a

[13] Y. Amani, S. Dancette, E. Maire, J. Adrien, and J. Lachambre, "Two-Scale Tomography Based Finite Element Modeling of Plasticity and Damage in Aluminum Foams," *Materials (Basel, Switzerland)*, vol. 11, no. 10, 2018. https://doi.org/10.3390/ma11101984

[14] J. Schukraft, C. Lohr, and K. A. Weidenmann, "2D and 3D in-situ mechanical testing of an interpenetrating metal ceramic composite consisting of a slurry-based ceramic foam and AlSi10Mg," *Composite Structures*, vol. 263, p. 113742, 2021. https://doi.org/10.1016/j.compstruct.2021.113742

[15] R. Füßel, M. Gude, and A. Mertel, "In-situ X-ray computed tomography analysis of adhesively bonded riveted lap joints," in *17th European Conference on Composite Materials*, Munich, 2016.

[16] F. Pottmeyer, J. Bittner, P. Pinter, and K. A. Weidenmann, "In-Situ CT Damage Analysis of Metal Inserts Embedded in Carbon Fiber-Reinforced Plastics," *Exp Mech*, vol. 57, no. 9, pp. 1411–1422, 2017. https://doi.org/10.1007/s11340-017-0312-0

[17] D. Köhler, R. Kupfer, J. Troschitz, and M. Gude, "Clinching in In Situ CT—A Novel Validation Method for Mechanical Joining Processes," in *The Minerals, Metals & Materials Series, NUMISHEET 2022: Proceedings of the 12th international conference and workshop on*, K. Inal, J. Levesque, M. Worswick, and C. Butcher, Eds., [S.l.]: SPRINGER, 2022, pp. 833–840.

[18] D. Köhler, R. Kupfer, J. Troschitz, and M. Gude, "In Situ Computed Tomography-Analysis of a Single-Lap Shear Test with Clinch Points," *Materials (Basel, Switzerland)*, vol. 14, no. 8, 2021. https://doi.org/10.3390/ma14081859